17. Gilbert, S. P., Webb, M. R., Brune, M. & Johnson, K. A. Pathway of processive ATP hydrolysis by kinesin. *Nature* **373,** 671–676 (1995).
18. Ma, Y. & Taylor, E. W. Kinetic mechanism of the kinesin motor domain. *Biochemistry* **34,** 13242–13251 (1995).
19. Leibler, S. & Huse, D. A. Porters versus rowers: a unified stochastic model of motor proteins. *J. Cell Biol.* **121,** 1357–1368 (1993).
20. Coppin, C. M., Finer, J. T., Spudich, J. A. & Vale, R. D. Detection of sub-8-nm movements of kinesin by high-resolution optical-trap microscopy. *Proc. Natl Acad. Sci. USA* **93,** 1913–1917 (1996).
21. Samuel, A. D. T. & Berg, H. C. Torque-generating units of bacterial flagellar motor step independently. *Biophys. J.* **71,** 918–923 (1996).
22. Block, S. M. & Svoboda, K. Analysis of high resolution recordings of motor movement. *Biophys. J.* **68,** 230s–241s (1995).
23. Duke, T. & Leibler, S. Motor protein mechanics: a stochastic model with minimal mechanochemical coupling. *Biophys. J.* **71,** 1235–1247 (1996).
24. Hackney, D. D. Evidence for alternating head catalysis by kinesin during microtubule-stimulated ATP hydrolysis. *Proc. Natl Acad. Sci. USA* **91,** 6865–6869 (1994).
25. Gelles, J. *et al.* Structural and functional features of one- and two-headed biotinated kinesin derivatives. *Biophys. J.* **68,** 276s–282s (1995).
26. Howard, J. The movement of kinesin along microtubules. *Annu. Rev. Physiol.* **58,** 703–729 (1996).
27. Peskin, C. S. & Oster, G. Coordinated hydrolysis explains the mechanical behavior of kinesin. *Biophys. J.* **68,** 202s–211s (1995).
28. Derenyi, I. & Vicsek, T. The kinesin walk: a dynamic model with elastically coupled heads. *Proc. Natl Acad. Sci. USA* **93,** 6775–6779 (1996).
29. Kull, F. J., Sablin, E. P., Lau, R., Fletterick, R. J. & Vale, R. D. Crystal structure of the kinesin motor domain reveals a structural similarity to myosin. *Nature* **380,** 550–555 (1996).
30. Block, S. M. Fifty ways to love your lever: myosin motors. *Cell* **87,** 151–157 (1996).

Acknowledgements. We thank S. Gross, W. Ryu, L. Satterwhite, M. Wang and especially K. Visscher for technical assistance and discussions; S. Gross for help in purifying kinesin; and P. Mitra and K. Svoboda for advice in the early stages of this project. This work was supported by a grant from NIGMS (S.M.B.) and predoctoral fellowships from NSF and American Heart Association (M.J.S.).

Correspondence should be addressed to M.J.S. (e-mail: schnitzr@princeton. edu).

Coupling of kinesin steps to ATP hydrolysis

Wei Hua*, Edgar C. Young, Margaret L. Fleming & Jeff Gelles

* *Biophysics and Structural Biology Graduate Program, Department of Biochemistry, and The Center for Complex Systems, Brandeis University, Waltham, Massachusetts 02254, USA*

A key goal in the study of the function of ATP-driven motor enzymes is to quantify the movement produced from consumption of one ATP molecule[1–3]. Discrete displacements of the processive motor kinesin along a microtubule have been reported as 5 and/or 8 nm (refs 4, 5). However, analysis of nanometre-scale movements is hindered by superimposed brownian motion. Moreover, because kinesin is processive and turns over stochastically, some observed displacements must arise from summation of smaller movements that are too closely spaced in time to be resolved. To address both of these problems, we used light microscopy instrumentation[6] with low positional drift ($< 39\,\mathrm{pm\,s^{-1}}$) to observe single molecules of a kinesin derivative moving slowly ($\sim 2.5\,\mathrm{nm\,s^{-1}}$) at very low (150 nM) ATP concentration, so that ATP-induced displacements were widely spaced in time. This allowed increased time-averaging to suppress brownian noise (without application of external force[4,5]), permitting objective measurement of the distribution of all observed displacement sizes. The distribution was analysed with a statistics-based method which explicitly takes into account the occurrence of unresolved movements, and determines both the underlying step size and the coupling of steps to ATP hydrolytic events. Our data support a fundamental enzymatic cycle for kinesin in which hydrolysis of a single ATP molecule is coupled to a step distance of the microtubule protofilament lattice spacing of 8.12 nm (ref. 7). Step distances other than 8 nm are excluded, as is the coupling of each step to two or more consecutive ATP hydrolysis reactions with similar rates, or the coupling of two 8-nm steps to a single hydrolysis. The measured ratio of ATP consumption rate to stepping rate is invariant over a wide range of ATP concentration, suggesting that the 1 ATP to 8 nm coupling inferred from behaviour at low ATP can be generalized to high ATP.

Box 1 Distribution of displacements observed with limited time resolution

Detection of processive motor steps can be modelled analytically. We assume that, in the absence of noise, every displacement detected has size nd_1, where n is a positive integer and d_1 is the unitary step size. We model the effects of a step discrimination method in which the time interval t between neighbouring unitary steps is detected only if $t >$ the time resolution, t_r. In this case, the probability that $n = 1$ is

$$P_1 = P(t > t_r),$$

where $P(t > t_r)$ is the probability that the interval $t > t_r$. The probability that $n = 2$ is the probability of not detecting the interval between one pair of unitary steps and detecting the interval between the next pair:

$$P_2 = \left[1 - P(t > t_r)\right]P(t > t_r) = (1 - P_1)P_1.$$

In general,

$$P_n = P_1(1 - P_1)^{(n-1)}.$$

The histogram of observed displacements will be:

$$H(x) = N' \cdot \begin{cases} P_{n'} & x = nd_1 \text{ with } n = 1, 2, 3, \ldots, \\ 0, & \text{elsewhere,} \end{cases}$$

where N' is the total number of displacements detected. N' also corresponds to the maximum value in the cumulative histogram,

$$C(d) = \int_0^d H(y)\,dy.$$

$C(d)$ differs from the cumulative histograms shown in Fig. 3, in that the latter include effects of experimental noise (see Methods). The total number of unitary steps $\tilde{N} = D/d_1$, where D is the total distance moved, and

$$\tilde{N} = N' \sum_{i=1}^{\infty} iP_i = N'/P_1.$$

At limiting ATP concentrations, mechanisms with the same d_1 but different coupling of steps to ATP hydrolysis give different $P(t > t_r)$ and therefore different histograms. For example, for a mechanism in which each unitary step is coupled to the hydrolysis of one ATP molecule,

$$P(t > t_r) = \mathrm{e}^{-(t_r/\tau)},$$

where $\tau = Td_1/D$ is the average time interval between steps, and T is the total time. In contrast, if each step is followed by two consecutive ATP hydrolysis events with rate constant ratio k,

$$P(t > t_r) = \frac{\mathrm{e}^{-[(k+1)t_r/\tau]} - k\,\mathrm{e}^{-[(k+1)t_r/k\tau]}}{1 - k}.$$

These results can be generalized to apply to mechanisms that include more than one unitary step size.

K448-BIO is a recombinant biotinylated protein containing the amino-terminal 448 amino acids of the *Drosophila* kinesin heavy chain (including the motor domain, which is sufficient for microtubule-based motility[8]). It forms stable dimers[9] and so, like intact kinesin[10], it contains two active sites. K448-BIO displays kinesin-like ATPase activity[9], and single dimers of K448-BIO attached to streptavidin beads move processively[11,12] (that is, for hundreds of nanometres without detaching from the microtubule), like intact kinesin[13,14] and other dimeric kinesin derivatives[15]. The rate of forward translocation by single molecules displays hyperbolic dependence on ATP concentration (Fig. 1a). The fitted Michaelis–Menten parameters from velocities at ATP concentrations $\geqslant 5\,\mu$M are confirmed by the slope of the linear ATP dependence of velocities at submicromolar ATP levels (Fig. 1a, inset). This strict hyperbolic dependence is consistent with a reaction sequence in which the two active sites of the enzyme bind ATP in a sequential manner, provided that an irreversible step, such as phosphate release, occurs between the two binding reactions. (A mechanism without an intervening irreversible step has a non-hyperbolic rate law[16].)

The ATP consumption associated with the motor's movement

can be quantified by comparing its single-molecule translocation velocity with its microtubule-activated ATPase rate measured in solution conditions at which all motor molecules are translocating[13]. We measured K448-BIO ATPase rates at maximally activating microtubule concentration. Over an ATP concentration range of 3–1,000 μM, the ATPase rate changes in parallel with the movement velocity (Fig. 1a), so that the 'coupling ratio' of ATP hydrolysis to distance moved is constant within experimental error (Fig. 1b). The value of the ratio corresponds approximately to one ATP hydrolysis for each 8.12 nm of forward translocation. However, the assumption that in the solution ATPase experiments all molecules are actively translocating may not be wholly accurate, as a normal active motor might spend a fraction of time in a 'quiescent' non-translocating state. The ratio observed probably excludes the consumption of high numbers of ATP molecules per 8 nm moved, or movement over many lattice spacings per ATP molecule, but may not be precise enough to distinguish, for example, whether the true coupling ratio is two ATP molecules per 8 nm, one ATP per 8 nm, or one ATP per 16 nm.

To characterize the coupling of kinesin movement to ATP hydrolysis by a complementary approach, we used video-enhanced differential interference contrast microscopy to follow with nanometre-scale precision[6] the movement of bead-labelled K448-BIO molecules on microtubules. K448-BIO moves in a series of discrete displacements rather like those observed in previous studies of intact kinesin[4,5]. At very low (150 nM) ATP concentrations, displacement events are well separated by dwell times (Fig. 2) and could be discriminated reliably by computer. The absence of applied force makes it unnecessary to correct displacement measurements for mechanical compliance[4,5], and eliminates concerns that applied load may alter the coupling mechanism[2]. Because the underlying unitary translocations ('steps') are stochastic, we expect that some groups of neighbouring steps may not be resolved and will give rise to displacements that are sums of the unitary step sizes. The number of unresolved steps (see Box 1) is significant when the time resolution of the step discrimination algorithm (~0.6 s) is not much less than the mean time between steps (2.5 s).

To take unresolved steps into account, we examined the size distribution of all detected displacements. This is valuable because this distribution will in general have a different shape for movement mechanisms with different step size, or with different coupling between ATP hydrolytic events and steps (Box 1). Another distinguishing factor is N, the total number of positive displacements observed in a given total time (T) and total distance (D) moved. A cumulative histogram of the displacements is a simple way of examining both of these features: the histogram shape shows distinctive features of the displacement distribution, and N is the histogram asymptote. We numerically simulated distance–time

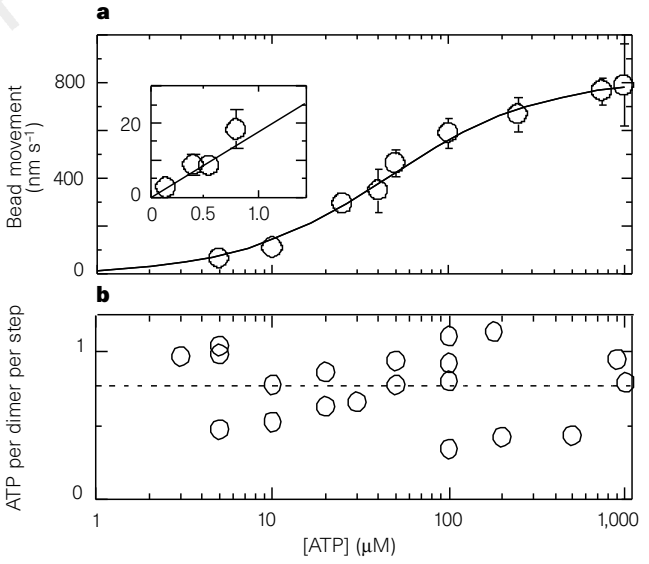

Figure 1 **a**, Velocities parallel to microtubule axis of beads of 100-nm diameter conjugated to single molecules of kinesin derivative K448-BIO. Points show mean velocities (±s.d.) from 6–40 observations at each concentration of ATP (with the exception of 0.55 μM ATP, where only one observation was made). Line shows least-squares fit to hyperbolic ATP dependence of all data collected at ATP concentration ⩾5 μM; the fitted values (±s.e.) for parameters were $V_{max} = 819 \pm 21$ nm s^{-1}, $K_m = 46.4 \pm 4.4$ μM. Inset, mean velocities at <5 μM ATP (linear concentration scale). **b**, ATP consumed by K448-BIO dimers per movement step assuming each step is the microtubule lattice spacing of 8.12 nm (ref. 7). For each ATP concentration, ATPase rate in solution at saturating microtubule concentration was expressed as turnovers per second per exchangeable nucleotide site and multiplied by 2 (because a translocating dimer must have two exchangeable sites). Single-molecule movement velocity at the same ATP concentration was calculated from the fit parameters from **a** and divided by 8.12 nm to express the rate as steps per second. Points show the ratio of hydrolysis rate to stepping rate: the horizontal line indicates the mean value of 0.77 ATP molecules per dimer per step (s.d. = 0.24, $n = 20$).

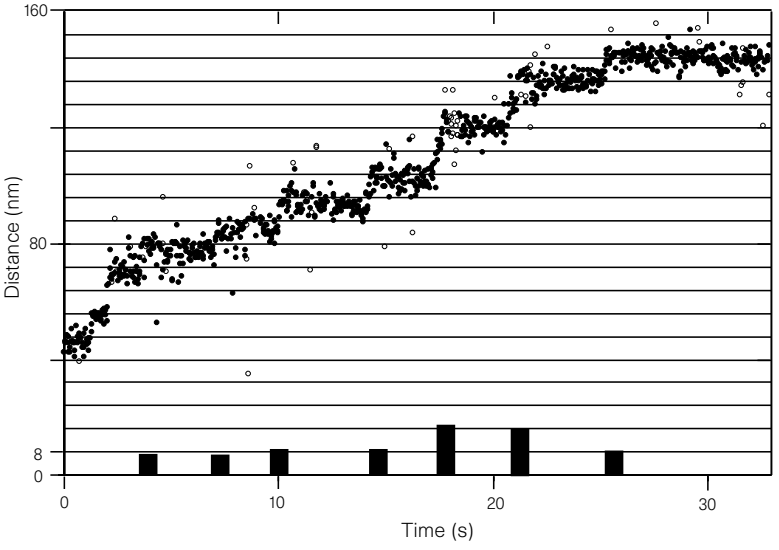

Figure 2 Movement of a bead-labelled single K448-BIO molecule along a microtubule in 150 nM ATP. Points mark the bead position on the microtubule axis; the time interval is 33 ms. Open circles represent measurements in which a free bead in solution diffused within one bead image diameter of the measured bead, possibly resulting in an inaccurate measurement. Bars indicate displacements detected in the same data record by an automated step-discrimination algorithm. The height of the bar represents the displacement magnitude, and its horizontal position represents the time of the event. The displacements near time 2 s were not detected by the algorithm because the first and last 1.98 s of the data record are excluded from the analysis (see Methods).

records for various coupling mechanisms and subjected them to the same step discrimination algorithm (that is, with the same time resolution for detection of displacements) as was used for experimental traces. The cumulative histogram of displacements from the simulation of each mechanism can be compared directly with the experimental histogram (Fig. 3). The experimental data are consistent with a simple mechanism for kinesin movement in which each ATP hydrolysis is coupled to a step from one tubulin dimer on the microtubule to the adjacent dimer along the same protofilament (the '8.12' mechanism), but not with several other proposed kinesin mechanisms that were consistent with our solution ATPase measurements.

Mechanisms with a single ATP hydrolytic event coupled to an average unitary step size of less than 8 nm will have a value of N (for a given D and T) higher than that in the '8.12' mechanism. This is illustrated in Fig. 3 by the '3–5–8' mechanism (random steps of 3, 5 and 8 nm with equal probabilities, as discussed in ref. 5, with each step coupled to a single hydrolytic event). The value of N is greater than that in the '8.12' mechanism because the average unitary step size (5.3 nm) is smaller. Furthermore, the shape of the displacement distribution is far from that of the experimental data, providing strong evidence against this mechanism. A similar mechanism with steps of 3 and 5 nm also fails to fit (Fig. 3).

The cumulative histograms also exclude mechanisms that postulate a constant step size of 8 nm but a coupling ratio different from that of the '8.12' mechanism. For the '1ATP/2step' mechanism, in which two steps of 8.12 nm are coupled to a single ATP hydrolytic event, the average time interval between the two steps ($\leqslant$10 ms to produce the 100 s^{-1} mean stepping rate at saturating ATP) is much less than the time resolution. This yields a small N because the behaviour is essentially identical to stepping with unitary step size of 16.24 nm. The '2ATP/step' mechanism, with an 8.12 nm step coupled to a pair of ATP hydrolytic events with identical rates, has, compared with the '8.12' mechanism, a larger proportion of time intervals between steps (Box 1) long enough to be resolved by the discrimination algorithm, and larger N. Mechanisms with one step coupled to more than two identical ATP hydrolysis reactions give a cumulative histogram (not shown) similar to that of the '2ATP/step' mechanism.

The data also exclude modified versions of the '2ATP/step' mechanism (not shown) in which one step is coupled to a pair of non-identical ATP hydrolysis reactions, unless the two productive ATP-binding events occur at rates that differ by a factor of $>$15. This difference in rates can occur only if the enzyme is capable of two distinct modes of ATP hydrolysis. No evidence for this unusual possibility has been found in studies of kinesin kinetics[17,18] so, although we do not discount it entirely, we consider it improbable.

The distribution of time intervals between observed displacements (not shown) is monoexponential, which is consistent with the '8.12' mechanism.

In summary, every displacement of 8 nm requires at least one ATP hydrolysis, and probably not more than one, so 8 nm is the distance associated with what can rightly be called a complete enzymatic cycle. In stable complexes of kinesin with a microtubule, kinesin interacts with only one tubulin dimer[19–22]. An 8-nm cycle can then be interpreted as reliable movement of kinesin from one tubulin dimer to the adjacent tubulin dimer of the same microtubule protofilament. This confirms the observation at high ATP concentration that kinesin molecules follow a single protofilament[6,11,23]. We do not exclude the possibility that at some point in the cycle kinesin makes a step with an apparent displacement different from 8 nm (such as the 5-nm displacements previously reported[5]). Nevertheless, we predict that in our experiments such steps must be part of a series of displacements that sum to 8 nm with each iteration of the ~10-ms cycle. Our data (temporal and spatial distribution of discrete movements, ATP dependence of movement velocity, and solution ATPase) are fully consistent with the tight coupling of ATP consumption to forward movement, and with the currently

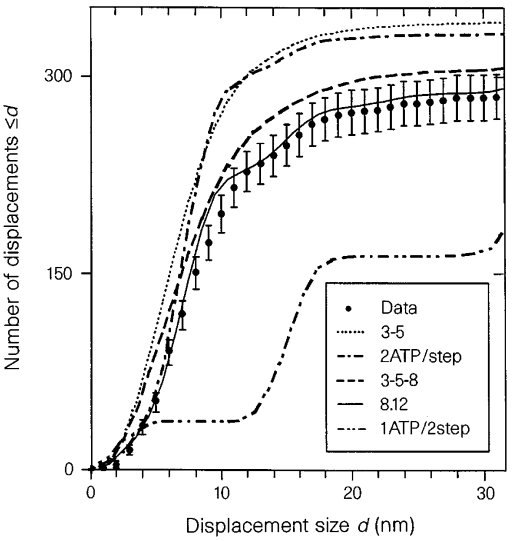

Figure 3 Cumulative histograms of displacements of bead-labelled enzyme compared to histograms calculated for various enzyme mechanisms. The number of positive displacements less than or equal to a displacement size d is plotted on the vertical axis. Points represent a histogram (±s.e.) of $N = 294$ observed positive displacements (negative displacements[4,5], 26 of which were >5.1 nm, were not included) from experiments at 150 nM ATP, with total bead movement distance $D = 2{,}678$ nm and total bead movement duration $T = 1{,}082$ s. Lines indicate simulated behaviour of various enzyme mechanisms. Note that the simulations have no adjustable parameters and are not fit to the experimental data. Each line is the average of data from 20 simulations, each with D and T identical to the experimental data record. The mean time between ATP hydrolytic events (t_{ATP}) was calculated from D and T and the properties of each mechanism. For the '8.12' mechanism, each hydrolytic event is coupled to a single step of 8.12 nm ($t_{ATP} = 3.28$ s, $N = 291$); '2ATP/step' mechanism, each 8.12 nm step is coupled to a pair of hydrolytic events ($t_{ATP} = 1.64$ s, $N = 332$); '1ATP/2step' mechanism, each hydrolytic event is coupled to a pair of 8.12-nm steps separated by 10 ms (8.12 nm divided by V_{max}; $t_{ATP} = 6.56$ s, $N = 193$); '3–5' mechanism, random 3- and 5-nm steps, with each step coupled to a single ATP hydrolytic event ($t_{ATP} = 1.64$ s, $N = 341$); '3–5–8' mechanism, 3-, 5- and 8-nm steps randomly mixed with equal probabilities and with each step coupled to a single hydrolytic event ($t_{ATP} = 2.15$ s, $N = 307$). The '8.12' mechanism is clearly the closest match to the data.

favoured 'alternating sites' mechanisms for kinesin movement[3,24]. The coupling ratio measured in the macroscopic steady-state experiments reflects its microscopic foundation, namely a regular 8-nm mechanochemical cycle that can be identified by direct observation of stochastic movements. □

Methods

Enzyme preparation and ATPase assay. K448-BIO was purified[9], supplemented with 1 M sucrose, frozen in liquid nitrogen, and stored at −80 °C. Taxol-stabilized microtubules were prepared as described[25]. ATPase assays were performed at 22–25 °C using radiolabelled nucleotide methods adapted from ref. 26: K448-BIO (0.2–0.7 μg ml^{-1}) was mixed with [α-^{32}P]ATP in reaction buffer (ABT buffer[11] supplemented with 2 mM dithiothreitol (DTT) and 0.1 mg ml^{-1} bovine serum albumin); reactions were started by adding 1.7–2.0 mg ml^{-1} microtubules. At each time point, a portion was quenched by a 5–6-fold dilution into ice-cold 1 M HCl spiked with unlabelled ATP and ADP standards; the mixture was neutralized with an equal volume of 1 M Tris base, filtered (Millipore Ultrafree-MC polysulphone, 30,000 NMWL), and chromatographed on TSK-GEL DEAE-2SW HPLC for quantification of labelled ATP and ADP. Corrections were made for impurities in the radiolabelled nucleotide stock[26]. ATPase rates were constant up to 15% completion of reaction; the rate from each enzyme–microtubule mixture was corrected by subtraction of the rate for microtubules alone and expressed as enzyme turnovers per second per exchangeable nucleotide binding site. Concentration of exchangeable nucleotide sites in K448-BIO preparations was measured[27] by incubating 3–9 μg ml^{-1} K448-BIO with 0.5–2 μM [α-^{32}P]ATP in reaction buffer supplemented with 0.1 mg ml^{-1} creatine kinase and 2 mM phosphocreatine. Creatine-kinase-inaccessible [^{32}P]ADP (that is, K448-BIO exchangeable nucleotide sites) in quenched portions of this mixture was determined as above. Accumulation of [^{32}P]ADP displayed kinetics similar to those of [^{32}P]ADP depletion after addition of 170 μM unlabelled ATP.

Motility assays. Streptavidin beads were mixed with K448-BIO at a ratio of 0.2–1.0 enzyme dimers per bead[11], and motility was measured (at 22–25 °C) as described[11], except that samples were supplemented with 2 mM DTT and ATP concentration was varied. Samples with <5 μM ATP were supplemented with 7 μg ml^{-1} creatine kinase and 2 mM phosphocreatine to prevent ATP depletion. As expected for beads driven by single kinesin molecules[14], beads typically detached from the microtubule before reaching the microtubule end (mean travel distances, 300–1,000 nm at 5–1,000 μM ATP). In most experiments, bead velocity was calculated from positions of video cursors manually superimposed on the bead image in video frames at the start and end of the movement episode. Data for mean velocity v at [ATP] ⩾ 5 μM were fitted to the Michaelis–Menten equation $v = V_{max}[ATP]/([ATP] + K_m)$ by least-squares regression (weighted by reciprocal of standard deviation). For nanometre-precision measurements of movement[11] at 0.15 or 0.8 μM ATP, carboxyl-polystyrene beads 100 nm in diameter were adsorbed to the coverslip surface (after microtubules) to serve as stationary reference points.

Nanometre-precision position measurements. We made simultaneous position measurements on multiple beads in the microscope field. Positions of moving beads were measured relative to the position of the coverslip determined from the averaged positions of ⩾10 stationary beads, to compensate for mechanical drift in the microscope[6]. The residual drift rate was <39 pm s^{-1} in both x and y in 8 independent measurements; precision[6] was 2.0 nm in x and 0.8 nm in y. Position on the microtubule axis is calculated by projecting the y position to the measured[11] microtubule orientation, which was always <2° from the y direction. Beads that moved <15 nm were excluded from further analysis. A free bead in solution diffusing within one image diameter of the measured bead intefered with ~6% of the position measurements (Fig. 2).

Step discrimination algorithm. Axial position records were smoothed with a recursive median filter[4,28] with rank 15 (495-ms window), the first derivative was calculated with a 14-point (462 ms) quadratic convolute[29], and the first and last 1.98 s of data were discarded. The beginning and end of bead dwell positions were taken as the crossings of a velocity threshold value of 6.1 nm s^{-1}. The magnitude of the displacement between adjacent dwells was calculated as the difference in mean dwell positions, with positive direction defined as the direction of the net movement in the data record. The algorithm was validated by demonstrating that, for all enzyme mechanisms discussed, its effect could be duplicated by a simple constant-parameter linear system (W.H. and J.G., unpublished results) in which those unitary steps separated by a time interval longer than a time resolution t_r are resolved, and those separated by a shorter interval are summed. This system shows the desirable properties that N is nearly independent of small changes in noise amplitude, but is approximately inversely proportional to unitary step size and stepping rate. For all mechanisms examined, N' (Box 1) changed in parallel with N.

Monte-Carlo simulations with added noise. To simulate the behaviour of different coupling mechanisms (Fig. 3), we generated traces each with displacements of the specified sizes separated by random time intervals chosen from an exponential or biexponential distribution. Data records (with standard deviations of 2.5, 3.3 and 3.6 nm; by comparison, the precision of the moving bead traces was ~3.8 nm) from control experiments in which 1 mM AMP-PNP was substituted for ATP were added to the generated traces to simulate experimental noise. Curves in Fig. 3 were produced by applying the step discrimination algorithm to traces. The variance of the cumulative histogram outputs from 20 independent simulations of the '8.12' mechanism is that expected from statistical variation alone, indicating that the discrimination algorithm does not introduce significant additional variance in the histograms.

Received 13 February; accepted 12 May 1997.

1. Taylor, E. W. Variations on the theme of movement. *Nature* **361,** 115–116 (1993).
2. Ishijima, A. *et al.* Single-molecule analysis of the actomyosin motor using nano-manipulation. *Biochem. Biophys. Res. Commun.* **199,** 1057–1063 (1994).
3. Hackney, D. D. Evidence for alternating head catalysis by kinesin during microtubule-stimulated ATP hydrolysis. *Proc. Natl Acad. Sci. USA* **91,** 6865–6869 (1994).
4. Svoboda, K., Schmidt, C. F., Schnapp, B. J. & Block, S. M. Direct observation of kinesin stepping by optical trapping interferometry. *Nature* **365,** 721–727 (1993).
5. Coppin, C. M., Finer, J. T., Spudich, J. A. & Vale, R. D. Detection of sub-8-nm movements of kinesin by high-resolution optical-trap microscopy. *Proc. Natl Acad. Sci. USA* **93,** 1913–1917 (1996).
6. Gelles, J., Schnapp, B. J. & Sheetz, M. P. Tracking kinesin-driven movements with nanometre-scale precision. *Nature* **331,** 450–453 (1988).
7. Beese, L., Stubbs, G. & Cohen, C. Microtubule structure at 18 Å resolution. *J. Mol. Biol.* **194,** 257–264 (1987).
8. Stewart, R. J., Thaler, J. P. & Goldstein, L. S. B. Direction of microtubule movement is an intrinsic property of the motor domains of kinesin heavy chain and *Drosophila* ncd protein. *Proc. Natl Acad. Sci. USA* **90,** 5209–5213 (1993).
9. Young, E. C., Berliner, E., Mahtani, H. K., Perez-Ramirez, B. & Gelles, J. Subunit interactions in dimeric kinesin heavy chain derivatives that lack the kinesin rod. *J. Biol. Chem.* **270,** 3926–3931 (1995).
10. Scholey, J. M., Heuser, J., Yang, J. T. & Goldstein, L. S. B. Identification of globular mechanochemical heads of kinesin. *Nature* **338,** 355–357 (1989).
11. Berliner, E., Young, E. C., Anderson, K., Mahtani, H. K. & Gelles, J. Failure of a single-headed kinesin to track parallel to microtubule protofilaments. *Nature* **373,** 718–721 (1995).
12. Berliner, E. thesis, Brandeis Univ. Waltham, MA (1995).
13. Howard, J., Hudspeth, A. J. & Vale, R. D. Movement of microtubules by single kinesin molecules. *Nature* **342,** 154–158 (1989).
14. Block, S. M., Goldstein, L. S. B. & Schnapp, B. J. Bead movement by single kinesin molecules studied with optical tweezers. *Nature* **348,** 348–352 (1990).
15. Vale, R. D. *et al.* Direct observation of single kinesin molecules moving along microtubules. *Nature* **380,** 451–453 (1996).
16. Segel, I. H. *Enzyme Kinetics* (Wiley, New York, 1975).
17. Gilbert, S. P., Webb, M. R., Brune, M. & Johnson, K. A. Pathway of processive ATP hydrolysis by kinesin. *Nature* **373,** 671–676 (1995).
18. Ma, Y.-Z. & Taylor, E. W. Mechanism of microtubule kinesin ATPase. *Biochemistry* **34,** 13242–13251 (1995).
19. Arnal, I., Metoz, F., DeBonis, S. & Wade, R. Three-dimensional structure of functional motor proteins on microtubules. *Curr. Biol.* **6,** 1265–1270 (1996).
20. Hirose, K., Lockhart, A., Cross, R. A. & Amos, L. A. Three-dimensional cryoelectron microscopy of dimeric kinesin and ncd motor domains on microtubules. *Proc. Natl Acad. Sci. USA* **93,** 9539–9544 (1996).
21. Hirose, K., Lockhart, A., Cross, R. A. & Amos, L. A. Nucleotide-dependent angular change in kinesin motor domain bound to tubulin. *Nature* **376,** 277–279 (1995).
22. Kikkawa, M., Ishikawa, T., Wakabayashi, T. & Hirokawa, N. Three-dimensional structure of the kinesin head–microtubule complex. *Nature* **376,** 274–276 (1995).
23. Ray, S., Meyhoefer, E., Milligan, R. A. & Howard, J. Kinesin follows the microtubule's protofilament axis. *J. Cell Biol.* **121,** 1083–1093 (1993).
24. Gelles, J. *et al.* Structural and functional features of one- and two-headed biotinated kinesin derivatives. *Biophys. J.* **68,** 276s–282s (1995).
25. Berliner, E. *et al.* Microtubule movement by a biotinated kinesin bound to a streptavidin-coated surface. *J. Biol. Chem.* **269,** 8610–8615 (1994).
26. Hackney, D. D., Malik, A.-S. & Wright, K. W. Nucleotide-free kinesin hydrolyzes ATP with burst kinetics. *J. Biol. Chem.* **264,** 15943–15948 (1989).
27. Hackney, D. D. Kinesin ATPase: rate-limiting ADP release. *Proc. Natl Acad. Sci. USA* **85,** 6314–6318 (1988).
28. Gallagher, N. C. Jr & Wise, G. L. A theoretical analysis of the properties of median filters. *IEEE Trans. Acoust. Speech Signal Process.* **29,** 1136–1141 (1981).
29. Savitzky, A. & Golay, M. J. E. Smoothing and differentiation of data by simplified least squares procedures. *Anal. Chem.* **36,** 1627–1639 (1964).

Acknowledgements. We thank X. Liu for preliminary studies, H. Mahtani for technical assistance, and C. Miller and H. Huxley for comments on the manuscript. This work was supported by the NIH and by an HHMI predoctoral fellowship to E.C.Y.

Correspondence and requests for materials should be addressed to J.G. (e-mail: gelles@binah.cc.brandeis.edu).